

Provided for non-commercial research and education use.
Not for reproduction, distribution or commercial use.



This article appeared in a journal published by Elsevier. The attached copy is furnished to the author for internal non-commercial research and education use, including for instruction at the authors institution and sharing with colleagues.

Other uses, including reproduction and distribution, or selling or licensing copies, or posting to personal, institutional or third party websites are prohibited.

In most cases authors are permitted to post their version of the article (e.g. in Word or Tex form) to their personal website or institutional repository. Authors requiring further information regarding Elsevier's archiving and manuscript policies are encouraged to visit:

<http://www.elsevier.com/copyright>



Contents lists available at ScienceDirect

Earth and Planetary Science Letters

journal homepage: www.elsevier.com/locate/epsl

Crustal growth along a non-collisional cratonic margin: A Lu–Hf isotopic survey of the Eastern Cordilleran granitoids of Peru

Aleksandar Mišković*, Urs Schaltegger

Department of Mineralogy, Earth Sciences Section University of Geneva, 13 rue des Marâchers CH 1205 Geneva, Switzerland

ARTICLE INFO

Article history:

Received 3 July 2008

Received in revised form 23 December 2008

Accepted 5 January 2009

Editor: R. W. Carlson

Keywords:

Hf
zircon
granitoids
Peru
crust
growth

ABSTRACT

An extensive *in situ* Lu–Hf isotopic study of zircon from the Eastern Cordilleran batholiths of Peru using laser ablation multi-collector inductively coupled mass spectrometry (LA-MC-ICPMS) reveals a systematic covariance between granitoid magma sources and tectonic regimes which shaped the proto-Andean margin of central Western Amazonia since > 1.15 Ga. The Hf isotope systematics are characterised by a range in initial $^{176}\text{Hf}/^{177}\text{Hf}$ compositions for a given intrusive event suggesting mixing of material derived from the Paleoproterozoic crustal substrate and variable addition of juvenile sources from Neoproterozoic to Cenozoic time. Intrusives associated with phases of regional compressive tectonism correspond to mean initial ϵHf values of -6.73 , -2.43 , -1.57 for the Ordovician (Famatinian), Carboniferous–Permian and Late Triassic respectively, suggesting a minimum crustal contribution between 40% and 74% by mass. The average initial Hf systematics from granitoids associated with periods of regional extension such as the middle Neoproterozoic, Permian–Triassic and Cenozoic Andean back arc plutonism are consistently shifted towards positive values (mean initial $\epsilon\text{Hf} = -0.7$ to $+8.0$) indicating systematically larger inputs of juvenile magma (25% to 38% of ancient crust by mass). In the absence of evidence for significant lateral accretion of exotic crust, the time integrated Hf record from the central proto-Andean margin of western Amazonia suggests crustal reworking was the dominant process during episodes of arc magmatism, implying that most crustal growth took place vertically via crustal underplating of isotopically juvenile, mantle derived melts during intervals of crustal extension.

© 2009 Elsevier B.V. All rights reserved.

1. Introduction

Accounting for the origin of continental crust is a challenging task due to: i) the complexity of petrogenetic processes that are required for the differentiation of primary basaltic magmas to produce bulk quartzofeldspathic compositions of average continental lithologies (Hildreth and Moorbath, 1988; Annen et al., 2006), ii) uncertainty in mass fluxes across the Mohorovičić discontinuity, including the pathways of primitive melts towards mid-upper crustal reservoirs (Reymer and Schubert, 1984), (Davidson et al., 2005), and iii) scant exposure and consequently limited knowledge of the composition and extent of the lowermost continental crust (Behn and Kelemen, 2006), (Rudnick and Gao, 2003). Despite these obstacles, the broad similarity in trace element budgets between bulk continental crust and island arc andesites (Nb, Ta, Ti anomalies and Ba, Rb, U, Th, K, and Pb enrichment) has led to the “island arc” or andesite” model for the origin of continental crust (Taylor, 1977). Indeed, the rate ($\sim 200 \text{ km}^3/\text{km arc length}/\text{Ma}$), and nature of

mechanisms proposed to operate along modern intra-oceanic arcs, namely two-stage melting, ascent and differentiation of underplated, asthenospheric mantle-derived melts above subducting oceanic lithosphere, followed by delamination of ultramafic cumulates from the overridding plate, have been largely successful in explaining both the volumes, and geochemistry of continental crust generated, at least during the Phanerozoic (Davidson and Arculus, 2005). Current models for the origin and stabilisation of cratons include orthogonal accretion of allochthonous crustal blocks along convergent plate margins (Bowring and Karlstrom, 1990), (Abbott and Mooney, 1995), coupled with the emplacement of granitoid batholiths that are, at least in part, composed of mantle-derived magmas (Rudnick, 1995). The extent to which this juvenile addition takes place in long-lived orogens is difficult to estimate by elemental abundances alone because sedimentary systems are efficient mixers of crustal detritus (i.e. sialic end-member), while melting to produce emblematic granitic batholiths tends to vertically average large domains of middle to lower crust and uppermost mantle (basaltic end-member) (Patchett and Samson, 2003). On the other hand, attempts at assessing juvenile additions by conventional Sr–Nd–Pb isotope systematics are only successful if sufficient isotopic contrasts exist between invading magmas and the country rock (Hildreth et al., 1991). Moreover, the contribution of mantle-derived melts to the

* Corresponding author. Current address: Earth, Atmospheric and Planetary Sciences, Massachusetts Institute of Technology, 77 Massachusetts Avenue Cambridge, MA 02139 USA.

E-mail address: miskovic@mit.edu (A. Mišković).

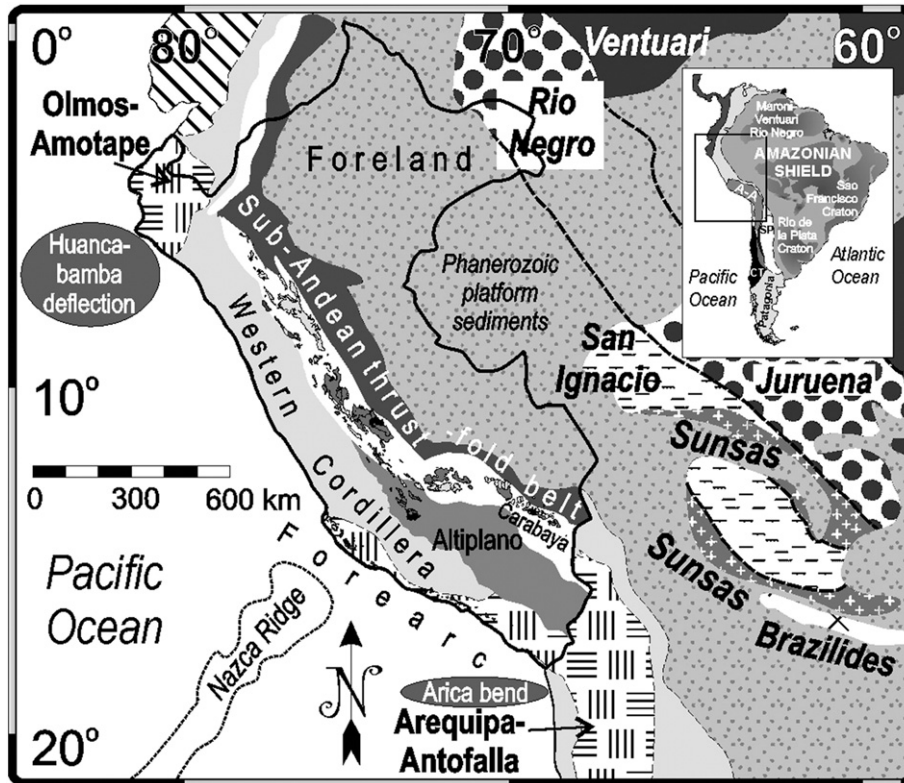


Fig. 1. Generalised tectonic map of the central Andes of South America showing the extent of the Eastern Cordilleran plutonism within the context of morphogeological belts of Peru. Intrusive colour scheme: Carboniferous–Permian (light grey); Permian–Triassic (dark grey); Late Triassic–Carabaya (hatched); Mesoproterozoic and Neoproterozoic (black). The index map shows tectonic provinces of Amazonia and the complex early Paleozoic accretionary assembly of the Chilean continental margin. Modified after Ramos and Aleman (2000), and Cordani and Sato (2000).

enlargement of continental crust along orogenic margins during episodes of extension is even less clear and has only recently received due attention (Albarède, 1998; Frost et al., 2001; Hollister and Andronicos, 2006).

The granitoid intrusives of the Peruvian proto-Andes however, intrude the ancient (1.1–2.5 Ga) continental crust of Western Amazonia,

display a range of isotopic signatures (Mišković et al., 2005), and are fortuitously situated along a segment of the cratonic margin that remained non-collisional, thus providing an ideal setting for a study of the importance of arc versus intra-plate magmatism in the formation of continental crust over an extended time period. We build upon the

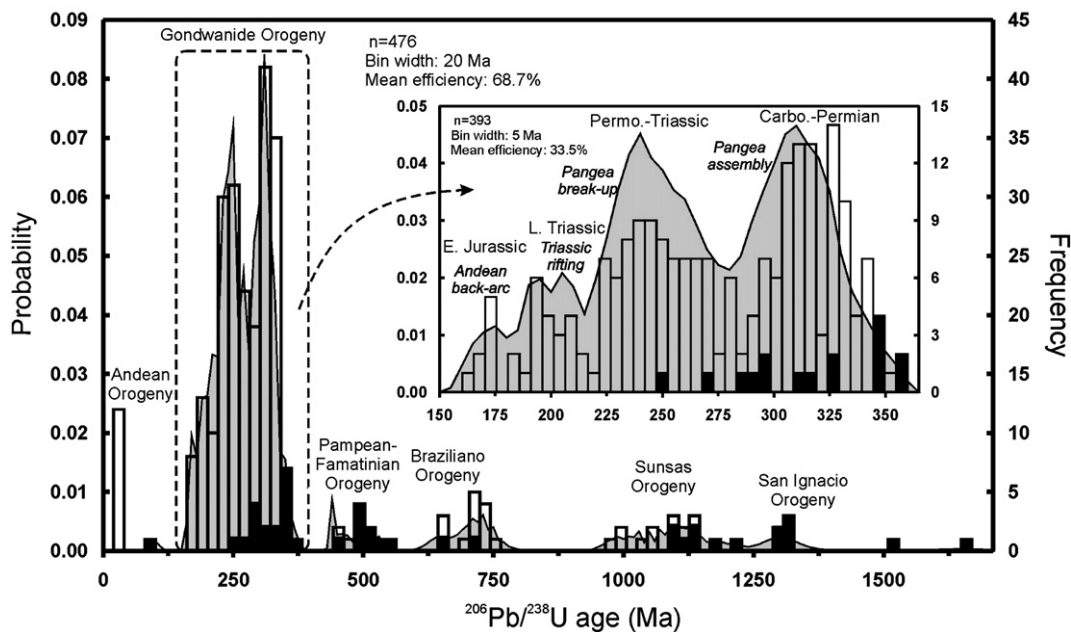


Fig. 2. Cumulative zircon $^{206}\text{Pb}/^{238}\text{U}$ age histograms summarising the known intrusive episodes of the Peruvian Eastern Cordillera granitoid. Inset displays the volumetrically most dominant plutonism of Gondwanide age (350–160 Ma). Empty bins represent crystallisation ages; black boxes correspond to the ages of inherited zircon cores.

results of an extensive geochemical characterisation and an *in situ* U–Pb geochronological study of igneous zircon from granitoid batholiths that form the backbone of the Eastern Cordillera of Peru (Mišković et al., 2009), and combine them with Lu–Hf isotopic tracing of dated zircon grains to identify the sources of consecutive magma pulses, and track crustal evolution of the proto-Andean margin of Western Amazonia during >1.0 G.y. Relating the secular changes in magma sources to the tectono-magmatic cycles of continental assembly and breakup along the Earth's longest lived active continental margin enables us to quantitatively constrain the relative magmatic contributions of six distinct Neoproterozoic and Phanerozoic tectono-magmatic episodes to the crustal architecture of a cratonic edge.

2. Regional setting

The Peruvian Eastern Cordillera (PEC) constitutes one of the five morphogeological belts of the central Andes. To the east, it is separated from west-dipping, Late Permian to Paleogene, continent-derived sedimentary rocks of the Sub-Andean fold-and-thrust belt by high-angle reverse faults, while to the west, it borders a 50 km wide, intra-cordilleran “High Plateau” composed of thick Mesozoic marine deposits north of 12°S, with the thickened Paleozoic to Mesozoic basement of the Altiplano to the southwest (Fig. 1). The Eastern Cordillera forms a wide anticline of early Paleozoic basal paraschists and phyllites belonging to, or contemporaneous with the poly-deformed Marañón Complex that was metamorphosed up to greenschist facies in four successive stages of deformation (Mégard, 1978). Although the ~110 Ma old Andean orogeny dominates the present form and lithologies of the Peruvian Western Cordillera (Ramos and Aleman, 2000), a majority of orogenic activity for at least 900 Ma has been focused along the Eastern Cordillera as the leading continental edge of Western Amazonia that preserved mineral relicts from basement lithologies as old as 1.67 Ga (Mišković et al., 2009).

2.1. Peruvian Eastern Cordilleran intrusives

The Eastern Cordilleran plutonic rocks emplaced into basement metasedimentary sequences between 6°S and 10°S belong to the diorite–tonalite–granodiorite–granite suite. They form a continuous 20–50 km wide intrusive belt with ages straddling the Carboniferous–Permian transition (336–285 Ma; Fig. 2) (Mišković et al., 2005). The granitoid intrusions are characterised by variable proportions of modal amphibole and biotite, and exhibit widespread textural evidence for the coexistence and mingling of compositionally contrasting magmas such as microgranular mafic enclaves, partially resorbed host feldspars and magmatic flame structures.

Voluminous, partially migmatized granitoids within the south-central segment of the Eastern Cordillera of Peru between 10°S and 13°S are Permian and Triassic in age (285–223 Ma; Fig. 2). This ~70 km wide intrusive belt is composed of K-feldspar megacrystic, biotite and subordinate amphibole bearing granodiorites that exhibit overall uniform silica enrichment compared to the northeastern Peruvian batholiths. The interior granitoid facies of each plutonic body includes mica-rich restites and subordinate mafic microgranular enclaves, whereas volumetrically minor biotite quartz monzonites occur along the margins of individual plutonic bodies. A unique feature of the central segment of the PEC is the existence of concordant Precambrian ages from two disparate localities. The emplacement of massive, biotite, quartz monzonites and alkali feldspar granites has been constrained to 752–691 Ma (Fig. 2). Closely associated with the Neoproterozoic granitoids are partially foliated, Late Mesoproterozoic to early Neoproterozoic tonalites and alkali feldspar granites, yielding ages from 1123 to 985 Ma, with a significant component of zircon inheritance between 1668 and 1305 Ma (Fig. 2) (Mišković et al., 2009). Triassic sinistral offset along an ENE–WSW trending transform fault system at 12.5°S, known as the Abancay deflection, is responsible for a

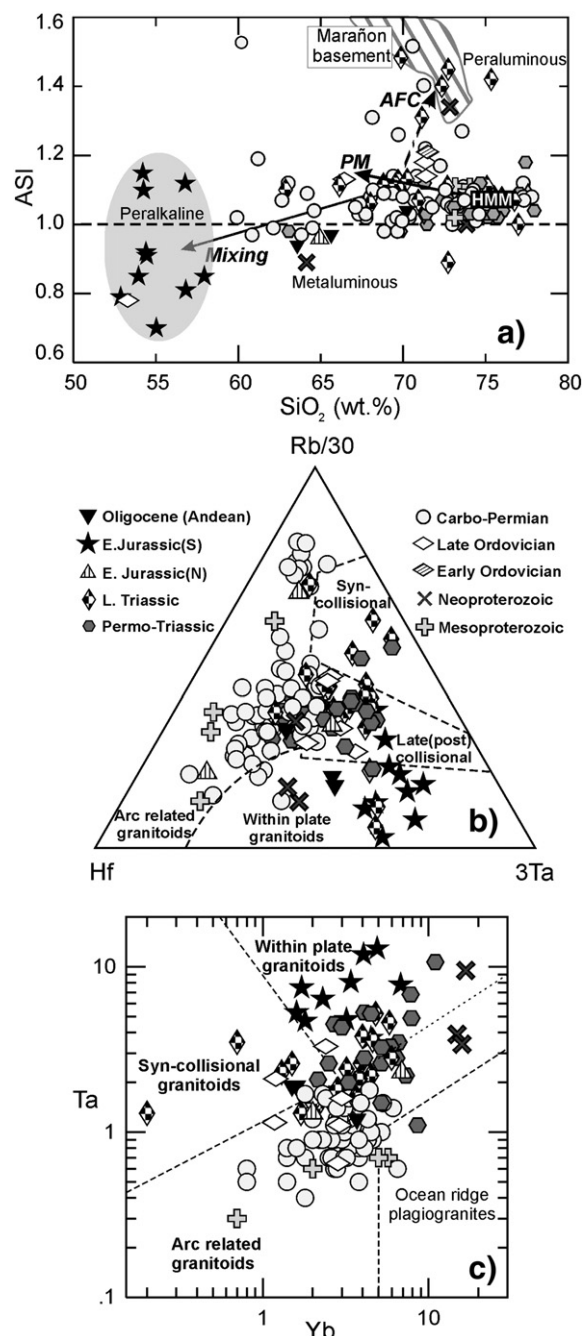


Fig. 3. Major and trace element chemistry of intrusive rocks of the Peruvian Eastern Cordillera; a) Alumina saturation index (mol. propr. $\text{Al}_2\text{O}_3/(\text{CaO} + \text{Na}_2\text{O} + \text{K}_2\text{O})$) plotted against silica enrichment as a rough proxy for the crustal source. Compositional trends generated by various petrogenetic processes are represented by arrows; AFC – assimilation-fractional crystallization or magma contamination by the basement, Marañón-type metasediments; PM – partial melting of the Ordovician granodioritic basement; Mixing – magma mixing with primitive dioritic melts; HMM – haplogranitic minimum melt; b) and c) Tectonic discrimination diagrams for the Peruvian Eastern Cordilleran granitoids based on chemically conservative HFS elements after Harris et al. (1986) and Pearce et al. (1984) respectively.

change in strike of the Eastern Cordillera and the resultant displacement of the intrusive belt by 200 km eastward (Carlotto et al., 2006; Fig. 1). At this latitude, two, medium grained, biotite-bearing, leucogranodiorite stocks were dated at 29.4 Ma and 31.4 Ma.

South of the orocline, Late Triassic–Early Jurassic (216–190 Ma) batholiths are composed of texturally homogeneous, medium-grained, biotite, alkali feldspar granites with a gradual increase in the proportion of modal mica southwards, and the first appearance of

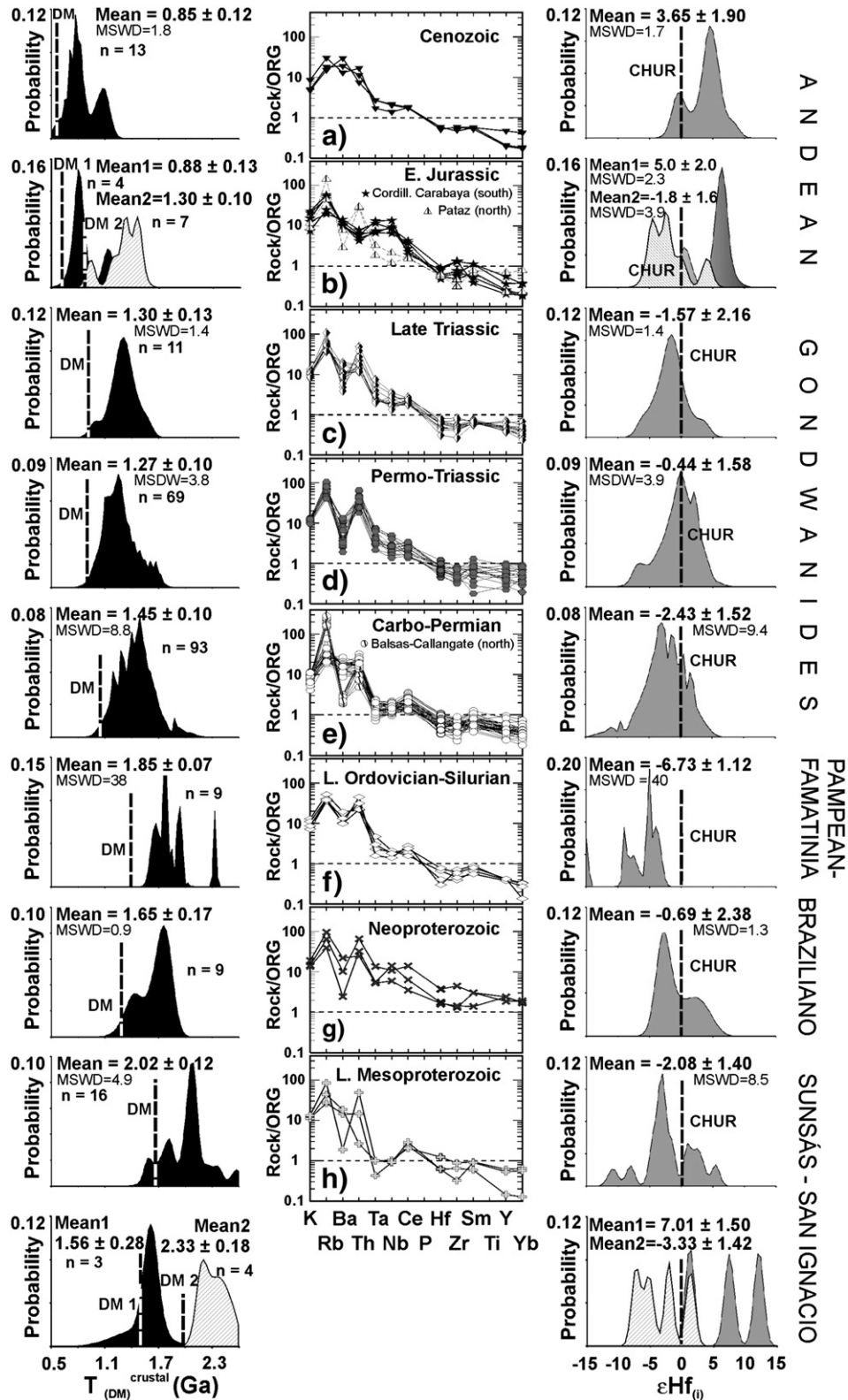


Fig. 4. Hf isotopic composition of zircon grains from the Peruvian Eastern Cordillera combined with trace element normalized patterns from Middle Cenozoic (a) to Mesoproterozoic (h). Left: Relative probability plots of crustal Hf model ages, where distance from the vertical bar representing the DM model ages correlates with an increase in source maturity. Centre: Ocean ridge granite (ORG)-normalised, selected trace element patterns for the Eastern Cordilleran intrusives. Normalising values taken from Pearce et al. (1984). Right: cumulative probability plots of ϵHf data with the vertical bar representing chondritic uniform reservoir (CHUR). Shaded areas correspond to plutonic pulses (Early Jurassic) and zircon inheritance (Early Mesoproterozoic) from the northern segment of Peruvian Eastern Cordillera.

muscovite in the monzo-granitoid assemblages of the southernmost Cordillera de Carabaya (Fig. 1). A single Late Ordovician concordia age of 446.5 Ma is recorded by a marginal, alkali feldspar granite of the

eastern Cuzco batholith. However, a coeval pulse of Early Paleozoic plutonism was also identified within the northeastern Peruvian Andes near 6°S, where partially metamorphosed Sitabamba granodiorites

yielded ages between 442 Ma and 445 Ma (Chew et al., 2007). Volumetrically minor but genetically important Jurassic peralkaline intrusives such as coarse grained, nepheline syenites of the Allincapac complex at 14 °S were intruded between 184 and 195 Ma in the Cordillera de Carabaya region, but also as 173 Ma, quartz-bearing syenites near the margins of the northern Carboniferous Pataz batholith at 8°S.

2.2. Geochemical constraints

Tabulated whole rock major, minor and trace element data are provided in the on-line supplementary material. The Early Jurassic Allincapac nepheline monzosyenites are the only sampled intrusives from the Eastern Peruvian Andes which are silica undersaturated and lack normative quartz. The Carboniferous–Permian, Ordovician and Late Triassic granitoids are all magnesian, but transgress boundaries between the calcic, calc-alkaline and alkali-calcic differentiation trends respectively (Miskovic et al., 2009). They span a wider compositional spectrum (60 to 77 wt.% SiO₂) than the predominantly alkali-calcic, magnesian to ferroan Neoproterozoic and Permo–Triassic plutons (70–78 wt.% SiO₂). In terms of aluminum saturation, the Eastern Peruvian granitoids are peraluminous to mildly metaluminous (molar Al₂O₃/CaO+Na₂O+K₂O; A/CNK=0.95 to 1.13). The exceptions are the strongly peraluminous Late Triassic Carabaya suite (A/CNK=0.98–1.42); volumetrically minor Oligocene metaluminous stocks (A/CNK=0.91–0.97), and the metaluminous to peralkaline Early Jurassic Allincapac nepheline bearing (alkali feldspar) syenites (Fig. 3a). Although primarily dependent on the differentiation history of silicic melts, trace element compositions of granitoids have long been used as first-order tectonic discriminators for granitoid sources (Barbarin, 1999). Trace element data from the Eastern Peruvian intrusives broadly corroborate genetic trends inferred from their major element chemistry. Multi-element, genetic classification plots (Harris et al., 1986; Pearce et al., 1984) clearly demarcate the arc affinities of the Carboniferous–Permian, Late Mesoproterozoic, and somewhat less convincingly, Ordovician granites of Peru (Fig. 3b,c). The Middle Neoproterozoic Permian–Triassic, Late Triassic and the southern Early Jurassic intrusives however, are classified as within-plate or syn-to-post tectonic suites, whereas the northern Jurassic and Oligocene plutons show mixed associations between intra-plate and continental arc-related granites. The oceanic plagiogranite normalised, multi-trace element plots (Pearce et al., 1984) for the Peruvian granitoids reveal a lack of heavy rare-earth element (HREE) fractionation characteristic of a garnet dominated source, and display an overall positive correlation between the extent of the large ion lithophile element enrichment (LILE/HFSE) and known episodes of subduction related magmatism. Negative Nb–Ta anomalies are observed in both the Late Mesoproterozoic plutons and within the Carboniferous–Permian suite, but are also mildly present in the Late Ordovician and Oligocene intrusive rocks (Fig. 4a, e, f, and h). In contrast, the Permo–Triassic, Early Ordovician quartz monzonite, and especially Neoproterozoic (monzo)granitoids, exhibit strong Ba/Th and Ba/Rb anomalies characteristic of anorogenic magmatism, in addition to the lack of a typical high LILE/HFSE trace element pattern associated with subduction (Fig. 4d, f, and g). However, such time-dependent, tectonic classification is occasionally complicated by the regional variability within coeval intrusive suites along the proto-Andean margin. For example, uniformly elevated high field strength (HFSE) elements that are characteristic of rift- or back arc-related plutonism displayed by the southern, Early Jurassic peralkaline nepheline syenites are markedly different from a mild subduction-zone trace element signature of the contemporaneous quartz syenites from the northern Pataz region (Fig. 4b). This may explain, the genetic ambiguity displayed by the Early Jurassic rocks in the tectono-discriminative, trace element plots in Fig. 3a and b. On a more local scale, the Early Mississippian, northern Balsas–Callangate pluton

shows considerably higher Rb/Ba values than the rest the Carboniferous–Permian plutonic belt (Fig. 4e). Given that the ratio of Rb/Ba decreases with increasing whole rock SiO₂ content, this trend cannot be explained by simple fractional crystallisation, but likely reflects an increased proportion of K-bearing phases in the source. The most recent (Oligocene) intrusive pulse is uniquely LILE enriched, with mildly depressed Nb–Ta concentrations indicative of a contaminated I-type magma that was emplaced marginally inboard of the principal arc batholiths (Walawender et al., 1990).

Taken together, major and trace element signatures allow for tectono-magmatic classification of the Eastern Cordilleran plutons into: i) Neoproterozoic anorogenic and transitional late- to post-orogenic granitoids of Permo–Triassic age; ii) Cordilleran-type, continental arc related intrusives from the Carboniferous to Permian, and Late Ordovician and Late Mesoproterozoic periods, iii) Late Triassic syn-collisional plutons and an Early Ordovician post-collisional intrusive, and iv) Early Jurassic within-plate, peralkaline plutons forming the cores of alkaline volcanic complexes, which are usually located in back-arc settings. The metaluminous granite porphyries of the modern Andean orogenic cycle that were emplaced in the Oligocene are magnesian, calcic and exhibit cationic ratios that overlap with those associated with continental arc settings.

3. Methodology

3.1. Hf systematics of zircon

As a common accessory mineral in granitoid rocks, zircon is readily used in studies of long-term magmatic evolution and orogen development (Kinny, 1986; Andersen and Griffin, 2004; Hawkesworth and Kemp, 2006). Its chemical and physical durability make it a robust repository for a range of radioactive nuclides and their radiogenic products (Finch and Hanchar, 2003). In addition to the three U–Th decay schemes utilised in zircon geochronology, a number of studies have since exploited complimentary ¹⁷⁶Lu–¹⁷⁷Hf and ¹⁴⁷Sm–¹⁴³Nd parent–daughter ratios as geochemical tracers (Patchett and Tatsu-moto, 1981; Corfu and Noble, 1992; Hanchar and Rudnick, 1995; Griffin et al., 2002). The strong affinity for Hf invariably produces very low Lu/Hf ratios in zircon (Lu/Hf ~0.005) regardless of coexisting mineral phases or environments. As such, the Lu–Hf systematics in zircon are comparable to those of the whole rock Sm–Nd system with both, the increased sensitivity to the juvenile magmatic component due to approximately twice the amount of the daughter element accumulated in the depleted mantle over similar geological times, and the ability to separate magmatic from inherited isotopic signals (Kinny and Maas, 2003). The introduction of multiple collector arrays to inductively coupled plasma source mass spectrometry (LA ICPMS) presently allows for a high degree of internal precision in Hf isotopic analyses. When coupled with *in situ* U–Pb geochronology of selected zircon domains by laser ablation ICPMS, this technique provides an unprecedented view into the timing and sources of magma generation.

3.2. Analytical techniques

Zircon was extracted from 58 intrusive samples using gravimetric and magnetic methods. Non-magnetic, euhedral and inclusion free grains between 50 and 200 μm in length were handpicked and a representative set was mounted in 1 cm thick epoxy blocks. The crystals were polished to reveal internal surfaces, and subsequently carbon coated. Cathodoluminescence (CL) imaging was done by the CamScan MV 2300 scanning electron micro-analyzer at the University of Lausanne under the operating conditions of 15 kV of accelerating potential and 15–20 nA beam current. The sample mounts were ultrasonically cleansed in a 5 vol.% HNO₃.

In situ measurements of Hf isotopes in zircon grains were carried out using a New Wave UP-213 Nd: YAG laser coupled to a Finnigan Neptune multi-collector ICP-MS at the University of Bergen. A laser with beam diameter of 20–28 mm was used at a rate of 10 Hz corresponding to energy densities between 5.56 and 3.56 J/cm². The laser beam was repeatedly scanned across the zircon surface confined to growth zones of uniform CL brightness, which were previously analysed for U–Pb geochronology, to ablate 100 μm long linear rasters to maintain signal stability. Gas blank was acquired for 35 s followed by 200 s of laser ablation. The typical signal intensities of ¹⁸⁰Hf varied between 0.40 and 0.65 V over 150–200 integration cycles, depending on duration. The ¹⁷⁶Hf/¹⁷⁷Hf, ¹⁷⁵Lu/176mass and ¹⁷³Yb/176mass data were corrected for gas blank and normalised to ¹⁷⁹Hf/¹⁷⁷Hf=0.7325 (Patchett and Tatsumoto, 1981), using an exponential correction for mass bias (Slama et al., 2008). Then, isobaric interferences of mass bias corrected ¹⁷⁶Lu and ¹⁷⁶Yb on ¹⁷⁶Hf, and ¹⁸⁰W on ¹⁸⁰Hf were corrected by measuring the intensity of the interference free ¹⁷⁵Lu, ¹⁷³Yb and ¹⁸²W isotopes, using the recommended values of ¹⁷⁶Lu/¹⁷⁵Lu=0.02668 (de Laeter and Bukilic, 2006), ¹⁷⁶Yb/¹⁷³Yb=0.7952 (Lapen et al., 2004), and ¹⁸⁰W/¹⁸²W=0.00452 (De Bièvre and Taylor, 1993) respectively, to calculate true ¹⁷⁶Hf/¹⁷⁷Hf ratios. The Plešovice natural zircon standard (Slama et al., 2008) was periodically analysed during this study and data were corrected for instrumental drift relative to the reference ¹⁷⁶Hf/¹⁷⁷Hf value of 0.282481±0.000013 (2 SD). The λ¹⁷⁶Lu decay constant of 1.930·10⁻¹¹ (Sguigna et al., 1982), and present CHUR values of ¹⁷⁶Hf/¹⁷⁷Hf=0.282772 and ¹⁷⁶Lu/¹⁷⁷Hf=0.0332 (de Laeter and Bukilic, 2006) together with the ²⁰⁶Pb/²³⁸U ages obtained from the LA ICP-MS zircon analyses were used to calculate the initial Hf and εHf values (Supplement Table 1). Depleted mantle model ages (*T*_{DM}) were calculated based on a model mantle source similar to average MORB with present-day ¹⁷⁶Hf/¹⁷⁷Hf=0.283251 (Nowell et al., 1998) and ¹⁷⁶Lu/¹⁷⁷Hf=0.0384 (Griffin et al., 2000). As they only represent minimum ages for the source of the host magmas, Hf *T*_{DM} ages are complemented by more realistic estimates of the protolith crustal residence in terms of the crustal model ages (*T*_{CR}^{Hf}), calculated by projecting the initial value of ¹⁷⁶Hf/¹⁷⁷Hf of a zircon to the depleted

mantle growth curve along a mean crustal ratio of ¹⁷⁶Lu/¹⁷⁷Hf=0.015 (Griffin et al., 2002).

Major, minor and selected trace element concentrations were determined by X-ray fluorescence (Supplement Table 2) on pressed powder pellets using a Phillips PW 2400 sequential spectrometer equipped with a rhodium tube at the University of Lausanne, Switzerland. A protocol developed by J. Michael Rhodes (University of Massachusetts, USA) and based on modified procedures of Norrish and Chappel (1967) and Reynolds (1967) was used for correction of non-linear background, inter-element interferences and variations in mass absorption (α coefficients and/or Compton scatter). The trace elements accuracy by the XRF method is ±5%. Fragments of the Li₂B₄O₇-diluted and fused glass discs were analysed for additional trace elements by laser ablation inductively coupled plasma mass spectrometry (LA ICPMS) at the University of Lausanne. The assembly consisted of a Perkin-Elmer ELAN 6100 quadrupole ICP mass spectrometer equipped with a dynamic reaction cell and coupled to a Lambda Physik 193 nm EXCIMER (ArF) laser that was fired at a frequency of 10 Hz delivering beam energies between 140 and 200 mJ. The trace element data were acquired by averaging three 80–120 mm analyses per disc (sample) over time intervals of 40–50 s on the peak transient signal and were repeatedly normalised to the NIST SRM 612 standard glass. Off-line data reduction of time-resolved signals was performed on a Lotus 123 macro (LAMTRACE) based spreadsheet package written by Simon Jackson of Macquarie University, Australia. The LA ICPMS REE data are accurate to within ±1% (La) or ±6% (Lu) on the basis of duplicate analyses. We have chosen to use Y, Zr, Nb, Sr, Rb, Ni, Cr, V, Ga, Co and Sc obtained by XRF, and the ICP-MS values for Ba, Ta, Hf, Cs, REE, Pb, Th, and U.

4. Results

Lu–Hf isotope data (εHf_i) from a total of 212 zircon grains are plotted relative to latitude of provenance in Fig. 5. The Hf isotopic composition and source model ages calculated for different intrusive periods through time are presented in chronological order in Fig. 6.

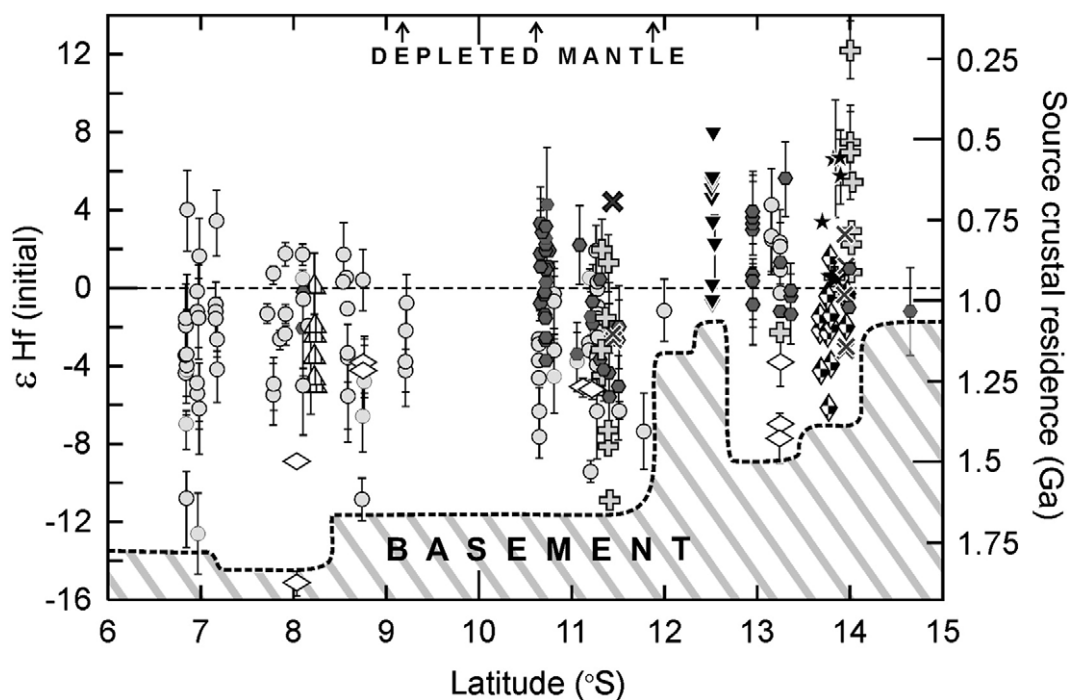


Fig. 5. Initial εHf values from the Peruvian Eastern Cordilleran batholiths plotted along orogenic strike. The Hf isotopic composition of mid-oceanic ridge basalts (i.e. depleted mantle – DM) is shown for reference. The Hf crustal model ages (Hf *T*_{DM}) are calculated using a ¹⁷⁶Lu decay constant of 1.93·10⁻¹¹ a⁻¹. Model ages assume an average crustal value of Lu/Hf=0.015 (Griffin et al., 2002). See Fig. 3 for the legend.

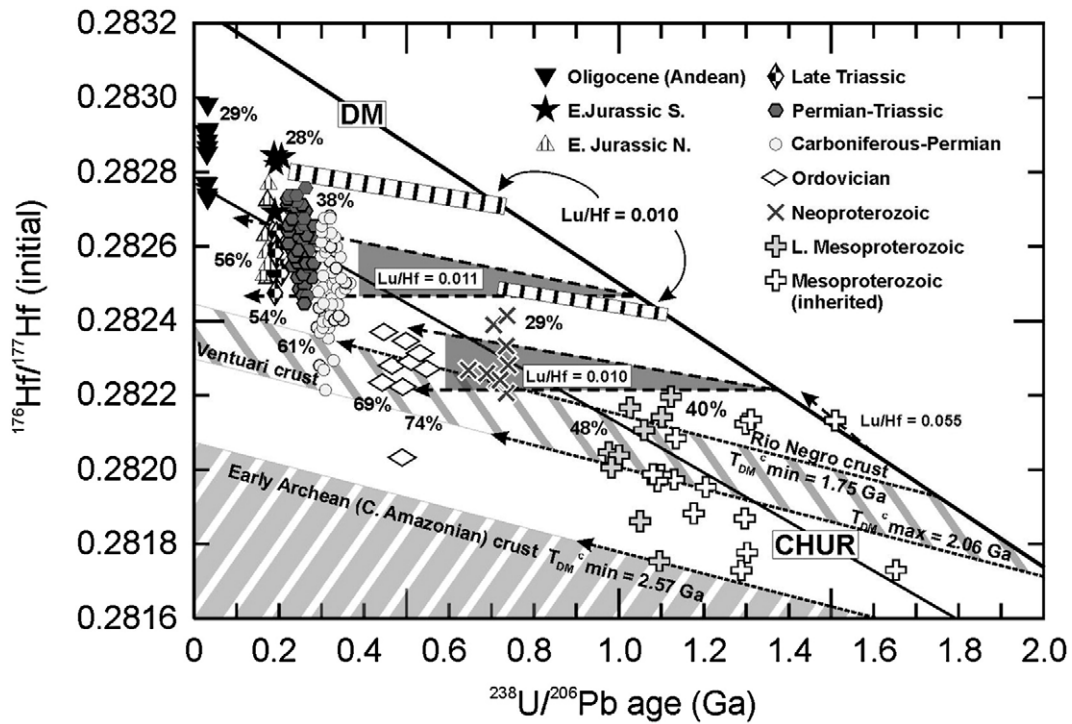


Fig. 6. Initial Hf isotopic composition of Eastern Peruvian intrusive zircon at times of crystallisation. The minimum limit of 1.75 Ga crust is defined by the growth curve with an average crustal $^{176}\text{Lu}/^{177}\text{Hf}$ of 0.015 projected from the most isotopically primitive Carboniferous–Permian zircon back to the Depleted Mantle (DM) evolutionary line. The maximum model age of the crustal end member that corresponds to the Ventuari tectonic province of north-central Amazonia is similarly defined relative to four Carboniferous–Permian outliers between initial $^{176}\text{Hf}/^{177}\text{Hf}$ ratios of 0.2822 and 0.2824. Likewise, the lower age limit of the crustal end member recorded by early Neoproterozoic and late Mesoproterozoic zircon grains (2.57 Ga) is defined by the most primitive 1.1 Ga crystallisation age. This is broadly coeval with the latest Archean segments of the Central Amazonian tectonic province. Possible single and multiple source models for the origin of the granitoids are shown in shaded areas and percentages respectively. $^{176}\text{Lu}/^{177}\text{Hf}=0.010$ represents the evolutionary trend of a possible Neoproterozoic juvenile end-member involved in the petrogenesis of Permian–Triassic aged zircon, while the extremely high Lu/Hf ratio of 0.055 for a single 1.51 Ga inherited zircon from the late Mesoproterozoic intrusive pulse is indicative of a garnet bearing either lower crustal or upper mantle residue extracted from the mantle at 1.6 Ga. Boxed Lu/Hf ratios relate to the required variations in the single source model that are necessary to explain Ordovician and late Triassic Hf systematics by invoking realistic, garnet-free crustal ratios of $\text{Lu}/\text{Hf} < 0.015$. The percent values indicate mass contributions of crustal end members in the binary source model for each of the plutonic pulses calculated at averaged emplacement times of 30, 175, 200, 245, 315, 455, 520, 715, 990, and 1075 Ma.

As is the case with zircon, the parent–daughter ratios of analysed grains from intrusives along the Eastern Cordillera were very low ($^{176}\text{Lu}/^{177}\text{Hf} < 0.0038$; Table 1). The Hf isotopic compositions at the time of crystallisation were nonetheless corrected for Lu decay, and span an overall ϵHf range of +8 to –9. Three Late Carboniferous xenocrystic zircon crystals and two analyses from the Late Ordovician intrusive episode plot significantly below the dominant, time-corrected zircon populations thus suggesting derivation from a substantially less enriched source (ϵHf initial = –11 to –15) than that of the bulk of coeval zircon grains. On the other hand, only one inherited grain from Mesoproterozoic in the Sunsás age Querobamba granite exhibits a depleted mantle composition with the initial $^{176}\text{Hf}/^{177}\text{Hf}$

$^{176}\text{Hf}/^{177}\text{Hf}=0.282134$, corresponding to ϵHf (initial) = +12 (Fig. 4). Despite the general uniformity of the Hf arrays relative to the CHUR evolution line, a closer examination reveals two dominant trends. There is a general decrease in the initial $^{176}\text{Hf}/^{177}\text{Hf}$ ratios relative to CHUR with time during the Precambrian from ϵHf of 7.0 ± 1.5 to -6.7 ± 1.1 (Fig. 4), which is followed by a systematic increase in radiogenic Hf through the Phanerozoic up to $\epsilon\text{Hf} = +3.7 \pm 1.9$, recorded by Oligocene plutons. Furthermore, alternating averages of ϵHf values that are observed throughout the sampled time span of 1.2 Ga show a systematic variation such that the Ordovician, Carboniferous–Permian, Late Triassic as well as the northern Early Jurassic intrusive pulses are shifted towards negative ϵHf initial values (–9 to +4), while the

Table 1
Mean magmatic Hf isotope signature of major orogenic events along the Peruvian Eastern Cordillera since 1.1 Ga

Orogenic episode	Tectonic regime	Age (Ma)	$^{176}\text{Lu}/^{177}\text{Hf}$	$^{176}\text{Yb}/^{177}\text{Hf}$	$^{176}\text{Hf}/^{177}\text{Hf}$	2 SE	$^{176}\text{Hf}/^{177}\text{Hf}(i)$	$\pm(2\sigma)$	$\epsilon\text{Hf}(i)$	$\pm(1\sigma)$	T_{DM} (Ma)	$\pm(1\sigma)$	T_{DM}^c (Ma)	$\pm(1\sigma)$
Late Andean	Continent. arc	30.4	0.00134	0.07092	0.28286	0.00005	0.28286	0.00005	3.76	0.94	545	37	842	58
Early Andean	Cont. arc (N)	171.0	0.00083	0.04587	0.28259	0.00005	0.28258	0.00005	-2.82	0.81	910	31	1356	50
Early Andean	Extensive (S)	180.5	0.00127	0.07554	0.28279	0.00006	0.28279	0.00006	4.68	1.01	636	39	904	63
L. Gondwanide	Anatexis-rift	202.1	0.00223	0.13563	0.28260	0.00006	0.28259	0.00006	-1.96	2.17	932	43	1328	67
Gondwanide	Extensive-rift	248.1	0.00162	0.08341	0.28262	0.00004	0.28261	0.00004	0.02	0.77	880	30	1243	98
E. Gondwanide	Continent. arc	316.3	0.00161	0.08678	0.28250	0.00005	0.28249	0.00005	-2.73	0.88	1046	34	1464	111
Famatinian Orogen	Continent. arc	453.9	0.00081	0.04166	0.28233	0.00006	0.28233	0.00006	-5.46	2.04	1251	78	1739	127
Pampean Orogen	Continent. arc	508.5	0.00193	0.10305	0.28232	0.00004	0.28230	0.00004	-5.19	1.36	1311	53	1765	93
pre-Braziliano	Extensive-rift	712.6	0.00085	0.05339	0.28230	0.00007	0.28229	0.00007	-0.69	2.39	1290	45	1648	167
Sunsás	Collisional	985.5	0.00141	0.06330	0.28206	0.00004	0.28203	0.00004	-3.61	1.41	1643	54	2040	109
Early Sunsás	Cont. arc (N)	1116.6	0.00162	0.08396	0.28197	0.00004	0.28194	0.00004	-3.96	1.32	1770	51	2163	107
Early Sunsás	Cont. arc (S)	1077.1	0.00145	0.07536	0.28219	0.00004	0.28216	0.00004	2.89	1.44	1472	55	1711	147
San Ignacio	Arc (N) inherit.	1296.3	0.00144	0.06612	0.28183	0.00004	0.28179	0.00004	-4.87	1.40	1955	27	2358	166
San Ignacio	Arc (S) inherit.	1305.7	0.00162	0.09224	0.28217	0.00006	0.28213	0.00006	7.25	1.99	1500	38	1619	159

Table 2
Average major element compositions of the Peruvian Eastern Cordillera intrusives relative to the (bulk) crustal elemental budgets

Age group	Oligocene	E. Jurassic (N)	E. Jurassic (S)	L. Triassic	Permo-Triassic	Carbo-Permian	Ordovician	Neoproterozoic	Mesoproterozoic	Wght. mean	UC	BC
n (samples)	3	3	23	26	48	86	5	3	5	202		
SiO ₂	67.11	70.82	56.51	71.64	69.43	66.05	70.35	70.78	66.52	66.76	67.97	64.2
TiO ₂	0.44	0.33	0.90	0.50	0.49	0.65	0.59	0.30	0.67	0.61	0.67	0.8
Al ₂ O ₃	16.46	14.99	19.80	14.36	14.81	15.80	14.81	14.17	14.87	15.76	15.40	14.1
FeO*	3.63	2.66	5.76	2.60	3.37	4.73	4.22	3.79	5.15	4.19	5.04	6.8
MnO	0.11	0.05	0.16	0.06	0.07	0.11	0.07	0.09	0.09	0.09	0.10	0.12
MgO	1.14	0.78	1.20	1.04	1.39	2.02	1.36	0.25	2.25	1.58	2.48	3.5
CaO	4.25	2.43	2.91	2.16	2.36	3.80	1.53	1.05	2.99	3.02	3.59	4.9
Na ₂ O	4.04	3.40	6.17	3.60	4.06	3.53	2.57	3.00	3.65	3.94	3.27	3.1
K ₂ O	2.48	4.36	5.94	3.77	3.72	2.99	4.20	6.34	3.50	3.70	2.80	2.3
P ₂ O ₅	0.19	0.08	0.28	0.17	0.13	0.17	0.15	0.04	0.10	0.17	0.15	0.18
Mg #	46.4	33.9	52.3	48.5	52.0	47.1	47.5	19.9	43.0	48.3	46.7	48.3
Hf (ppm)	5	8	9	4	6	5	4	21	17	7	5.12	4.71

Major elements are shown in weight percent oxide recast to 100% anhydrous.

Total FeO* = FeO + (Fe₂O₃ · 0.8998).

Molar Mg # = [MgO] / ([MgO] + [FeO*]).

Crustal estimates from Gao et al. (1998). UC = Upper continental crust; BC = Bulk continental crust.

Permian–Triassic, southern Jurassic, Oligocene and to a lesser extent Neoproterozoic granitoids exhibit a more juvenile character (ϵHf initial = −5.5 to +8).

The calculated crustal Hf model ages from the eastern Peruvian granitoids (T_{DM}) span two distinct Proterozoic time periods (Table 1; Fig. 4). The south-central, pre-Carboniferous intrusives of the PEC define a spectrum from 1.5 Ga to 2.1 Ga with five inherited zircon grains exhibiting T_{DM} ages of 2.2 Ga to 2.5 Ga, while the plutons emplaced during the Carboniferous to Jurassic show a population peak which temporally overlaps with the broadly defined Sunsas orogenic cycle (1.4–1.0 Ga). Moreover, the Hf isotopic record is spatially variable from north to south along more than 1200 km of orogenic strike, with the least enriched Hf values from the six transects varying from $\epsilon\text{Hf} = -13$ to -1 between latitudes of 7°S and 14.5°S (Fig. 5). Excluding data outliers, zircon grains with the lowest radiogenic Hf isotopic compositions correspond to a difference of ~0.5 Ga in the minimum source crustal residence times of basement from the northern Balsas pluton (1.6–1.7 Ga) to the southernmost Limbani stock near the Bolivian border (1.0–1.05 Ga), possibly reflecting the intrinsic age heterogeneity of the underlying crust. The shift towards more juvenile basement appears to be localised north of the Abancay deflection at 12.5 °S with a substantial decrease in minimum crustal residence times between 12°S and 13°S from 1.5 to 1.0 Ga. The Abancay orocline appears to regionally truncate the baseline trend of 1.5 Ga source residence times for the south-central PEC intrusives with a moderate increase in source residence times of 0.3 Ga to ~1.25 Ga south towards the Cordillera de Carabaya (Fig. 5).

5. Discussion

Jaillard et al. (2000) have shown that the tectonic history of the central Andes is simpler than the dominantly accretionary tectonics of both the northern Andes of Ecuador and Colombia (Spikings et al., 2001; Vallejo et al., 2006) and the Chilean orogenic extension (Miller and Söllner, 2005; Rapalini, 2005). Indeed, notwithstanding the brief episode of accretion and removal of the Paracas block in the Ordovician, central Western Amazonia is unique in having persisted as an active continent–ocean margin without significant lateral addition of crust for at least 700 Ma. Considering that the PEC intrusives represent time averaged equivalents of the upper continental crust (Table 2), and closely approach the bulk crustal composition (Gao et al., 1998), assessing the involvement of crust and mantle derived magmas in the petrogenesis of Peruvian granitoids implicitly measures their relative contributions to crustal growth along a non-collisional cratonic margin.

5.1. Isotopic models

Two genetic models are employed to replicate the observed isotopic variations, and quantify the involvement of the ancient basement. Our single source scenario assumes partial melting of isotopically heterogeneous (lower) crustal reservoirs with uniform age extracted from a depleted mantle source at times of known juvenile magmatism (Andersen et al., 2007). By allowing for the Hf isotopic evolution of such crust along variable, yet realistic $^{176}\text{Lu}/^{177}\text{Hf}$ ratios, it is possible to replicate isotopic arrays that are characterised by relatively restricted $^{176}\text{Hf}/^{177}\text{Hf}$ ratios (Fig. 6). Alternatively, the Hf isotopic ratios recorded by suites exhibiting wider zircon spectra can be expressed in terms of two-component mixing of melts between an (upper) crustal reservoir and depleted mantle. We consider the global depleted mantle (DM) as a juvenile end-member (mean Hf = 2.31 ppm; Kelemen et al., 2003), and allow for progressively younger crustal reservoirs during the Late Mesoproterozoic (2.57 Ga), Neoproterozoic (2.06 Ga), and post-Devonian plutonism (1.75 Ga). These ages (T_{DM}) are defined by the intersection of the DM line with the $^{176}\text{Lu}/^{177}\text{Hf}$ vector of 0.015 projected from the least enriched zircon of each of the three pulses. Given the geochemical evidence for derivation from a lower crustal protolith however, the two anorogenic to post-orogenic plutonic pulses in the middle Neoproterozoic and Permo–Triassic time are modeled relative to lower crustal end members. In the absence of garnet, such lower crustal sources would evolve along mildly lower Lu/Hf ratios of 0.01 since the separation from the source at 750 Ma and 1.1 Ga respectively (hatched rectangles in Fig. 6). Mean crustal contributions to each magmatic event are computed by averaging the $^{176}\text{Hf}/^{177}\text{Hf}$ spectra in Fig. 6, using the formalism above, and assuming upper crustal Hf concentrations (Hf = 5.12 ppm; Gao et al., 1998). Although being dependent on the choice of end-members, and based on globally averaged elemental concentrations of the continental crust, this model provides first-order quantitative estimates of the relative participation of crust and mantle in the petrogenesis of continental margin granitoids since the Mesoproterozoic.

5.1.1. Single source model

The single component model can be successfully applied to two PEC intrusive pulses that exhibit most prominent zircon inheritance thus suggesting their petrogenesis as dominantly crustal melts (Mišković et al., 2009). The Cambro–Ordovician intrusive episode can be modeled by invoking a source with a minimum model age equivalent to the middle Mesoproterozoic San Ignacio orogeny (1.35–1.40 Ga; Boger et al., 2005). To obtain the total range of $^{176}\text{Hf}/^{177}\text{Hf}$ observed in these early Paleozoic zircon grains, a variation in

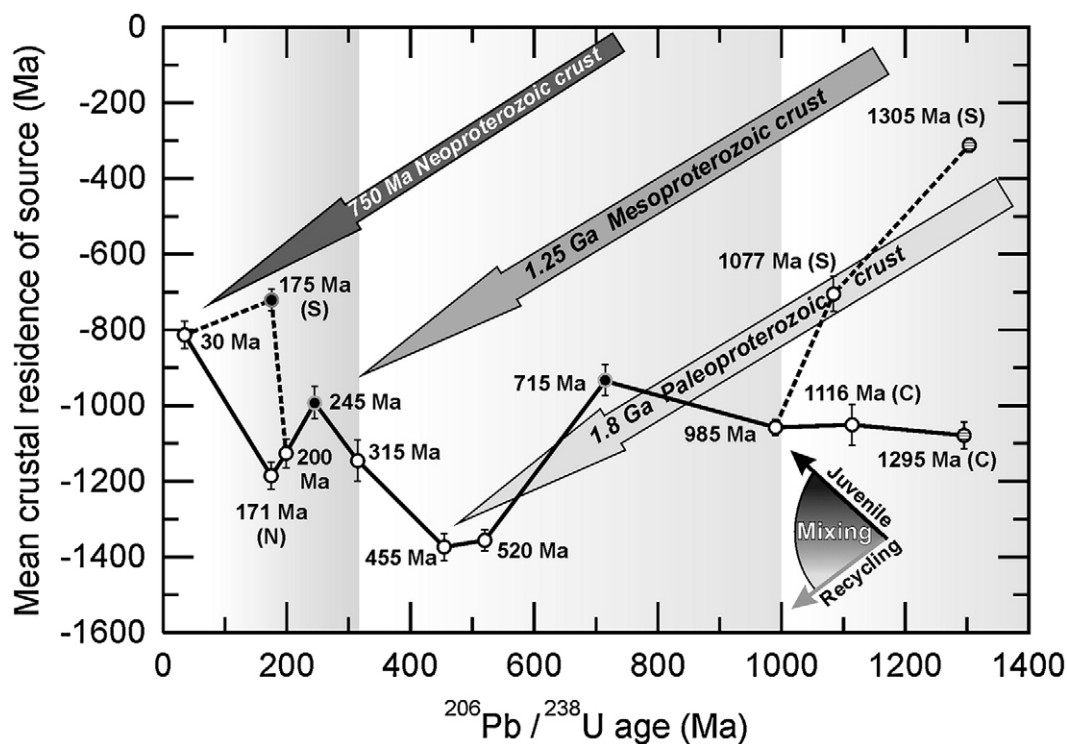


Fig. 7. Event signature curve for the Peruvian segment of the proto-Andean margin of Western Amazonia based on Hf and U–Pb systematics in PEC plutonic zircons following the *TerraneChron* methodology (Belousova et al., 2006). Mean crustal residence time of plutonic protoliths ($T_{DM}^c_{source} - T_{magma\ crystallisation}$) is plotted versus the average $^{206}\text{Pb}/^{238}\text{U}$ age of each intrusive episode. An upward trend with decreasing age suggests juvenile input, while a downward trend implies reworking of older (basement) crust. Vertical bars show variance of the Hf crustal residence times ($T_{DM}^c_{max} - T_{DM}^c_{min}$) in Ma for each intrusive event. Shaded backgrounds correspond to a Wilson cycle interval since assembly of Rodinia at ~1.0 Ga and Pangea at 0.31 Ga. Open and filled symbols relate to periods of arc-related and extension-related magmatism respectively, while hatched circles represent inherited magmatic signatures; (N) – northern PEC; (C) – central PEC; (S) – southern PEC.

$^{176}\text{Lu}/^{177}\text{Hf}$ ratio of ≤ 0.01 is needed over a time span between 0.88 and 0.95 Ga. Similarly, the Hf isotopic composition of the Carabaya intrusive zircon grains which crystallised during the Late Triassic intrusive event can be replicated by assuming a minimum age of the source to be coeval with the peak Sunsás orogenic activity at 1.05 Ga ago, and allowing 850 Ma of isotopic evolution with $^{176}\text{Lu}/^{177}\text{Hf} \leq 0.011$. In both cases the maximum Lu/Hf ratios are well within the average values for depleted continental crust devoid of garnet (Lu/Hf > 0.03). This observation further corroborates the uniformly flat HREE patterns exhibited by granitoids from both intrusives episodes that exclude garnet bearing sources. It is interesting to note that minimum times of mantle extraction for the two magma sources overlap in time with periods of orogenic climax that were characterised by pervasive metamorphism and deformation. Consequently, the 1320–1337 Ma high grade deformational event that resulted in the Chiquitania para-gneisses of eastern Bolivia, and the 1020–1049 Ma Nova Brasilândia amphibolite facies metamorphism of the western Brazilian Rondônia province could have isotopically homogenised juvenile sources, which evolved isotopically for 800–900 Ma and were subsequently tapped during Phanerozoic plutonism (Geraldes et al., 2004; Wu et al., 2007). In the single component model, the apparently shorter residence time of magma sources which produced the southern Cordillera de Carabaya granitoids, relative to the northerly Cambro–Ordovician zircon population, confirms the south-younging trend of Andean crustal protoliths inferred from the Hf model ages (T_{DM}^c ; Fig. 5). The single source basements are in fact located on opposite sides of the sharp transition in Hf crustal model ages from 1.7 Ga to 1.2 Ga, positioned immediately north of the Abancay deflection. This further strengthens the argument that the region adjacent to this orocline may represent a major tectonic boundary between crustal domains

underlying present Peru (Petford et al., 1996). Our Hf crustal model ages suggest that this orogenic feature may date back to the Grenville–Sunsás orogeny as the inherent western Amazonian structure dividing crustal domains affected by San Ignácio and Sunsás tectonism respectively. The presence of inherited Phanerozoic magmatic zircon grains (NAM-27a and CAM-54; Table 1) that are characterised by extremely unradiogenic $^{176}\text{Hf}/^{177}\text{Hf}$ ratios, and hence characterised by long Hf crustal model ages in the PEC plutons, point to the presence of even older, middle to Late Paleoproterozoic crust below the westernmost margin of the craton; 850 to 1150 km away from the nearest Rio Negro-Juruena (1.5–1.8 Ga) and the Central Amazonian (Ventuari-Tapajos; 1.8–2.0 Ga) outcrops (Fig. 1; index map).

5.1.2. Binary source model

Intrusives emplaced during periods of extensional tectonism along the Peruvian cratonic margin show systematic excursions towards more enriched compositions in the two-component Hf isotopic space. The Early Jurassic, Permo–Triassic and Neoproterozoic pulses indicate between 25% and 38% of “mature” crustal input by mass while on the other hand, magmatism during convergent episodes, in all cases but the volumetrically trivial Oligocene stocks, carries a predominantly crustal signature (40–74 mass %). The spread of isotopic arrays observed in Fig. 6 indicates a progressive, but regionally realistic increase in the age of crustal end-members from 1.75 Ga for post-Devonian to ~2.5 Ga for the Sunsás-age plutons. Involvement of the Paleoproterozoic crust with Hf T_{DM}^c between 1.7 and 2.1 Ga in the genesis of the middle Neoproterozoic and the Phanerozoic Peruvian intrusives agrees with documented cases of Proterozoic crustal reworking elsewhere west of the Amazonian craton (Cordani and Sato, 2000). Lucassen et al. (2004) calculated comparable amount of assimilation of the metamorphosed Proterozoic basement in the

source of Late Paleozoic granites between 36°S and 41°S of the Chilean Pacific margin. Likewise, Nd isotope modeling of the Mississippian continental arc (Pataz) batholith in the northeastern Peruvian Cordillera resulted in up to 70% addition of ancient crustal material (1.43–2.06 Ga; Macfarlane et al., 1999). Given the evolved chemical compositions, high LILE contents and crustally matured whole-rock isotopic signatures, this would suggest that arc derived plutonism along the central proto-Andes generally reworked, assimilated and mixed with the upper crustal lithologies by a combination of MASH (Hildreth and Moorbath, 1988), and AFC processes (DePaolo, 1981), whereas the extension related magmas evolved from their juvenile sources relatively uncontaminated. The isotopic difference seen in our data could be fundamentally related to variations in crustal thickness that characterise compressional versus extensional tectonic regimes. In the former, compressed and thickened crust impedes the ascent of mantle derived magmas to allow for more hybridisation at the base, or within arc crust, which ultimately renders them isotopically evolved (Davidson and Arculus, 2005). Nonetheless, a distinction must be made between the intervals of fully developed continental arc plutonism such as the Carboniferous–Permian phase, and mostly anatectic compressional events that produced volumetrically minor intrusions, as was the case during the Ordovician and Late Triassic. Although predominantly “crustal”, the plutons belonging to the former group occasionally show juvenile inputs of up to +4 ϵ Hf units, whereas the former population is entirely unradiogenic and lies below ϵ Hf=CHUR (Fig. 5).

The negative excursions in ϵ Hf during episodes of arc plutonism leave open a possibility of source contamination by upper crustal sediments associated with subduction erosion along the proto-Peru–Chile trench. However, in the case of the well exposed Carboniferous–Permian arc magmatism for example, it is difficult to envisage how subducted sediments alone could have significantly contributed to an overall non-radiogenic Hf isotopic signature of the most voluminous magma flare-up along the central Andes since Mesoproterozoic. Namely, low sediment input along the modern Peru–Chile trench (6.18 km³ Ma⁻¹·km⁻¹; Rea and Ruff, 1996) reflects an arid climate that might have locally prevailed for the last 150 Ma (Hartley et al., 2005), albeit extensive forearc erosion is documented below the Lima Basin offshore central Peru since middle Eocene at the average rate of 109 km³ Ma⁻¹·km⁻¹ (Clift et al., 2003). If projected to proto-Andean episodes of arc magmatism, even such an extensive crustal input from the subduction erosion as recorded during Cenozoic would not significantly offset the source isotopic signature of Phanerozoic arc granitoids given the absence of isotopically mature cratonic material north of the Arequipa–Antofalla terrane 14°S since middle Ordovician (Mišković et al., 2009). Moreover, most of the subducted sediments along the modern Peru–Chile trench currently undergo low temperature dehydration reactions while residing in the forearc position and not below the arc axis *sensu stricto*, thus resulting in a thoroughly serpentinised forearc mantle wedge (Graeber and Asch, 1999). Combined with the evidence that incompatible trace element ratios of subducted continental detritus do not correlate well with those of arc magmas at modern low-flux margins (<0.32 Mg·a⁻¹·cm⁻¹ or 12.8 km³ Ma⁻¹·km⁻¹; Plank, 2005), it is safe to conclude that the bulk of the crustal signature observed in the eastern Peruvian arc-derived plutonic rocks must have been acquired by some means other than *en masse* source contamination (Ducea and Barton, 2007).

5.2. Implications for the crustal evolution of central Western Amazonia

A convenient way of viewing crustal evolution along Western Amazonia, as recorded by the Eastern Cordilleran plutons of Peru, is the event signature curve (Fig. 7; Belousova et al., 2006). The Late Mesoproterozoic–Early Neoproterozoic history of the margin was characterised by alternating phases of hybridisation of two reservoirs:

a more evolved, less enriched Hf crust in the north, and a more juvenile reservoir in southern Peru. The bimodal Hf isotope composition of zircon grains older than 1.0 Ga contrasts with the relatively homogeneous population in younger rocks, indicating that subsequent magmatism effectively homogenised initially contrasting isotopic signals. Following juvenile additions during the middle Cryogenian, a period of dominant crustal assimilation lasted until the early Paleozoic (Pampean and Famatinian Orogeny). The continual trend towards more juvenile isotopic compositions occurred throughout the Phanerozoic except for 50 Ma of compressive tectonism between the Late Triassic and Middle Jurassic. Here too a discrepancy is noted between crustal reworking in the northern Peruvian back arc, and the southern, isotopically juvenile nepheline syenites of the Allinacpac Complex, which in this case is probably more a consequence of differential thickness of the lithosphere after Permo–Triassic rifting than an intrinsic isotopic heterogeneity. The significance of the post-180 Ma period lies in the fact that although operating in concert over more than one Wilson cycle (break-up of Rodinia; assembly and break up of Pangea), the relationship between the episodes of subduction-related arc activity and a decrease in the juvenile magmatic component breaks down during the modern Andean orogenic cycle. The increase in the initial ¹⁷⁶Hf/¹⁷⁷Hf record during the Mid-Cretaceous to Late Paleogene period compared to the Proterozoic and Paleozoic plutons must be viewed however, in the light of the spatial position of the PEC in the middle to late Phanerozoic, with most of the arc plutonism occurring along the Peruvian Coastal batholith (Atherton and Petford, 1996). The granitic stocks emplaced during the Andean orogeny along the central Eastern Cordillera of Peru seem to represent relatively sporadic and volumetrically negligible pulses of magmatism emplaced inboard of a continental arc.

The long-term trend in crustal residence times agrees with the findings from the northern Chilean segment of the western Amazonian margin in that, although being a major site of magmatic activity during the Sunsás cycle, and especially during the assembly and breakup of Pangea, the central Andean margin of Amazonia did not experience appreciable crustal growth during the last 1.0 Ga (Franz et al., 2008). From the isotopic evidence, it appears that significant juvenile inputs probably took place only when the temporarily thinned continental margin was underplated by upwelling asthenospheric mantle and ponded basaltic melts. Haschke and Günther (2003) have documented ~2.6 km of basaltic underplating during 12 Ma of Late Cretaceous transpression in the northern Chilean Andes that contributed ~50 vol.% to crustal thickening. Similarly, structurally balanced cross-section in the northern and southern edges of the Peruvian Altiplano–Puna plateau between 9°S and 12°S revealed a relatively thick crust that coincides with foreland shortening of less than 30% (Kley and Monaldi, 1998), thus requiring additional processes to thicken the lithosphere such as magmatic additions to the lower crust (Lamb and Hoke, 1997). Considering that the central part of the PEC is occupied by the isotopically juvenile Permo–Triassic granitoids, the crustal thickness observed in this part of the orogen may correspond to significant additions of relatively juvenile magmatic material to the crustal budget. One of the reasons why neither the overall Phanerozoic increase in source juvenility, nor protracted Permo–Triassic plutonism resulted in net crustal growth may be due to the requirement that lower crustal gabbroic cumulates and restites must be returned (“recycled”) to the mantle via delamination, thus leaving behind the appropriate bulk chemistry (Arndt and Goldstein, 1989; Jull and Kelemen, 2001). Seismic reconstructions of the orogenic architecture in central Peru however, place the Moho at 60 km below the Eastern Cordillera, and its ~15 km thick upper crustal granitoid column (Dorbath, 1996). If the ultramafic complement to the evolved upper crust remained intact, as appears to be the case under the present Western Peruvian Andes (Coastal Batholith and Cordillera Blanca; Couch et al., 1981; Polliand et al., 2005), it may account for the absence of the net lithospheric growth as suggested by the Hf isotope systematics.

5.3. Global perspective and comparisons

There is currently little consensus regarding the dominant processes that are responsible for the enlargement and stabilisation of cratons, with the debate becoming progressively speculative with increasing ages of the crustal segments under scrutiny. The problem is exacerbated in part by the lack of exposure of geochemically comparable lithologies within the rock record, as well as comparisons of disparate cratonic blocks with often markedly different tectonic evolutions. While few studies challenge the importance of the genesis of juvenile continental crust at modern Island arcs such as the Izu–Bonin–Mariana system (Takahashi et al., 2007), it is less clear to what extent these crustal tracts have contributed to continental growth through time. Even if we ignore problems that spreading back arc basins may create in the dynamics of intra-oceanic arc accretion, it has been quantitatively shown that in some cases, crustal addition by juvenile arc-related magmatism can be entirely balanced through tectonic erosion or sediment loss to the trench (Scholl and von Huene, 2007). Moreover, solutions to terrestrial Pb paradoxes, where upper crustal and mantle Pb isotopic compositions plot in the future along the $^{207}\text{Pb}/^{204}\text{Pb}$ vs. $^{206}\text{Pb}/^{204}\text{Pb}$ growth curve, demand that crustal recycling along subduction zones has been a dominant process since the Middle Paleoproterozoic (Kramers and Tolstikhin, 1997). Despite these difficulties, accretionary tectonics involving lateral addition of juvenile island arc crust during the (Neo) Proterozoic is seen as the principal contributor to the growth of most of western North America, and the Arabian–Nubian Shield (Whitmeyer and Karlstrom, 2007; Harris et al., 1993). Alternatively, the dominant style of growth along the North China craton, the Linzizong segment of the Tibetan plateau and the Central Asian Orogenic Belt (CAOB) during middle to late Phanerozoic is attributed to either juvenile syncollisional felsic magmatism, or vertical accretion accomplished by underplating of basaltic magma (Mo et al., 2008; Yang et al., 2008; Jahn, 2004). The Sr–Nd isotopic trends from granitoids rocks in the CAOB, for example, yield between 60 and 100% of a mantle component in their petrogenesis (Jahn, 2004), and the Mesozoic granitoids of the North China craton record a significant input of juvenile melt, resulting from the removal of lithospheric mantle by asthenospheric upwelling during extension that was possibly associated with rollback of the Pacific plate (Yang et al., 2008).

The crustal residence times of granitoid protoliths from the PEC suggest divergent modes of crustal evolution between the Phanerozoic and Neoproterozoic. The event signature curve (Fig. 7) does not imply net crustal growth along the Peruvian Gondwanan margin over this time span because the effects of alternating arc and intra-cratonic related magmatism largely cancel out, although there is an observable positive slope to the trend of mean Hf residence time of granitoid protoliths between ~700 Ma and 520 Ma, followed by a reversal up to ~250 Ma. It appears that crustal reworking of the 1.8 Ga old Amazonian basement was a dominant process along this segment of the proto-Andean margin of Western Gondwana during Neoproterozoic, while juvenile magmatic additions seem prevalent in the middle and late Phanerozoic. On a global scale, these results contrast with the coeval juvenile Nd–Sr isotopic ratios obtained from the Arabian Shield accretionary collage, which is thought to be responsible for a significant proportion of global crustal budget generated during the Pan-African orogeny (700–550 Ma; Harris et al., 1993). A caveat to the apparent contradiction is the position of these cratonic margins relative to the focal point of super-continental assembly in the late Neoproterozoic. While Arabia witnessed repeated accretion of island arcs during the closure of the Mozambique Ocean (640–610 Ma), and eventual merger with African cratons into Eastern Gondwana (Meert, 2003), western South America (i.e. Western Gondwana) interacted with a gradually widening Iapetus Ocean as an active, yet non-collisional margin (Chew et al., 2008). Here, arc magmatism largely reworked the crustal substrate of the overriding

plate margin between 650 and 550 Ma as seen in the steep positive slope of the event signature curve (Fig. 7). The Permian–Triassic juvenile plutonism and the mafic, isotopically primitive component of the Carboniferous–Permian intrusives of the PEC however, are mostly in accordance with isotopic trends from global Mesozoic granitoid provinces such as the CAOB as well as the observed increase in mantle-derived Pb isotopic component in W-bearing mineral occurrences worldwide (Chiaradia, 2003). Nonetheless, the importance of a given granitoid pulse as a net contributor to crustal growth along a cratonic margin must be judged against the competing mechanism of juvenile accretion that may be operating regionally, and often contemporaneously. Indeed, this was the case along much of the neighboring Chilean margin of Gondwana in Phanerozoic. During the Famatinian Orogenic Cycle (480–440) for example, the Peruvian segment of the margin was characterised by the emplacement of granitoids with isotopic signatures showing the highest proportions of assimilated mature crust, while 1800 km southwards along orogenic strike, the NW Argentinean Puna experienced considerable growth by accretion of the Famatina Terrane, a composite island arc of Ordovician age (Ramos and Aleman, 2000). Both the global Neoproterozoic and regional Phanerozoic examples from Western Gondwana however, emphasise the combined importance of accretion of juvenile crustal blocks (intra-oceanic arcs) and marginal intra-cratonic magmatism over *in situ* arc magmatism during the enlargement of continental crust.

6. Conclusions

The integrated major chemistry and Hf isotopic record of the Peruvian Eastern Cordilleran batholiths indicate that both continental arc magmatism and tectono-thermal events associated with compression reworked the pre-existing crust. Orogenic episodes partially melted the predominantly Paleoproterozoic, mid-lower crustal substrate equivalent to the Rio Negro–Jurruena (1.5–1.8 Ga) and the Ventuari–Tapajos (1.8–2.2 Ga) tectonic provinces of the western Central Amazonian craton, which were subsequently assimilated or mixed with successive batches of subduction derived magmas. Consequently, the initially sharp boundaries between middle to late Proterozoic tectonic domains, as indicated by Hf isotopic parochialism over the orogenic strike, seem to have been obliterated by juvenile magmatic inputs and crustal reworking. Our tectono-magmatic model is a departure from a commonly held view of the importance of subduction-related magmatism in the evolution of continental crust, at least as it applies to continental arcs. It attributes crustal growth along the proto-Andean accretionary margin of Peru to tectonic phases dominated by regional extension, as the isotopically juvenile, mantle derived magmas underplated previously attenuated continental crust, and gave rise to either A-type (Neoproterozoic), or post-orogenic, transitional S-type granitoids (Permian–Triassic anatectites). The long-term Hf isotopic record suggests that arc magmatism along such non-accretionary cratonic margins may fundamentally be a distillation process, whereby relatively primitive lower crustal and mantle-derived melts mainly provide heat for extensive mid-to-upper crustal anatexis. However, the absence of net crustal growth by magmatism at PEC corroborates models that envisage addition of allochthonous juvenile crust as the principal mechanism for cratonic enlargement along long-lived orogens.

Acknowledgements

Daniel Kontak and Allan Clark are thanked for donating samples from the Cordillera de Carabaya. Cathodoluminescence micro-imagery was conducted at the University of Lausanne. *In situ* LA (MC) ICPMS Lu–Hf analyses at the University of Bergen, Norway was conducted with the able assistance of Jan Košler. This research was supported by the Swiss National Science Foundation.

Appendix A

Mass balance calculation in the binary source Hf isotopic mixing model was formulated as follows:

$$\frac{^{176}\text{Hf}}{^{177}\text{Hf}}_{\text{zircon}} = \frac{^{176}\text{Hf}}{^{177}\text{Hf}}_{\text{crust}} f_{\text{crust}} + \frac{^{176}\text{Hf}}{^{177}\text{Hf}}_{\text{DM}} (1 - f_{\text{crust}});$$

where f is the mixing parameter expressing the abundance of the crustal end member in the mixture.

To calculate the crustal mass contribution (m) to the melt from which a zircon crystallised, the absolute Hf concentrations of both reservoirs must be taken into account, yielding:

$$f_{\text{crust}} = \frac{\text{Hf}_{\text{crust}} \cdot m_{\text{crust}}}{(\text{Hf}_{\text{crust}} \cdot m_{\text{crust}}) + (\text{Hf}_{\text{DM}} \cdot m_{\text{DM}})}, \text{ and by rearranging we obtain:}$$

$$m_{\text{crust}} = \left(\frac{f_{\text{crust}} \cdot \text{Hf}_{\text{DM}}}{\text{Hf}_{\text{crust}} - f_{\text{crust}} \cdot \text{Hf}_{\text{crust}}} \right) \cdot m_{\text{DM}}.$$

If we define $k = \frac{f_{\text{crust}} \cdot \text{Hf}_{\text{DM}}}{\text{Hf}_{\text{crust}} - f_{\text{crust}} \cdot \text{Hf}_{\text{crust}}}$ and let $m_{\text{DM}} = 1$, then the mass percentage of the crust in the melt is given by the expression $F_{\text{crust}} \% = \left(\frac{k}{1+k} \right) \cdot 100$.

Appendix B. Supplementary data

Supplementary data associated with this article can be found, in the online version, at doi:10.1016/j.epsl.2009.01.002.

References

- Abbott, D., Mooney, W., 1995. The structural and geochemical evolution of the continental crust: support for the oceanic plateau model of continental growth. *Geophys. Res.* 33, 231–242.
- Albarède, F., 1998. The growth of continental crust. *Tectonophysics* 296, 1–14.
- Andersen, T., Griffin, W.L., 2004. Lu–Hf and U–Pb isotope systematics of zircons from the Storgangen intrusion, Rogaland Intrusive Complex, SW Norway: implications for the composition and evolution of Precambrian lower crust in the Baltic Shield. *Lithos* 73, 271–288.
- Andersen, T., Griffin, W.L., Sylvester, A.G., 2007. Sveconorwegian crustal underplating in the southwestern Pennoscandia: LAM-ICPMS U–Pb and Lu–Hf isotope evidence from granites and gneisses in Telemark, southern Norway. *Lithos* 93, 273–287.
- Annen, K., Blundy, J.D., Sparks, R.S.J., 2006. The genesis of intermediate and silicic magmas in deep crustal hot zones. *J. Petrol.* 47, 555–539.
- Arndt, N.T., Goldstein, S.L., 1989. An open boundary between lower continental crust and mantle: its role in crust formation and crustal recycling. *Tectonophysics* 161, 201–212.
- Atherton, M.P., Petford, N., 1996. Plutonism and the growth of Andean crust at 9°S from 100 to 3 Ma. *J. South Am. Earth Sci.* 9, 1–9.
- Barbarin, B., 1999. A review of the relationships between granitoid types, their origins and their geodynamic environments. *Lithos* 46, 605–626.
- Behn, M.D., Kelemen, P.B., 2006. Stability of arc lower crust: insights from the Talkeetna arc section, south central Alaska, and the seismic structure of modern arcs. *J. Geophys. Res.* 111, B11207. doi:10.1029/2006JB004327.
- Belousova, E.A., Reid, A.J., Griffin, W.L., O'Reilly, S.Y., 2006. Proterozoic rejuvenation of the Archean crust tracked by U–Pb and Hf-isotopes in detrital zircon. *Geochim. Cosmochim. Acta* 70, A44.
- Boger, S.D., Raetz, M., Giles, D., Etchart, E., Fanning, C.M., 2005. U–Pb age data from the Sunsas region of Eastern Bolivia, evidence for the allochthonous origin of the Paragua Block. *Precambrian Res.* 139, 121–146.
- Bowring, S.A., Karlstrom, K.E., 1990. Growth, stabilization and reactivation of Proterozoic lithosphere in the southwestern United States. *Geology* 18, 1203–1206.
- Carlotto, V., Tintaya, D., Cárdenas, J., Carlier, G., Rodríguez, R., 2006. Fallas transformates Permo-Triásicas: La falla Patacancha-Tamburco (sur del Perú): Resúmenes XIII Congreso Peruano de Geología, pp. 256–258.
- Chew, D.M., Schaltegger, U., Košler, J., Whitehouse, M.J., Gutjahr, M., Spikings, R.A., Mišković, A., 2007. U–Pb geochronologic evidence for the evolution of the Gondwanan margin of the north-central Andes. *Geol. Soc. Amer. Bull.* 119, 697–711.
- Chew, D.M., Magna, T., Kirkland, C.L., Miskovic, A., Cardona, A., Spikings, R., Schaltegger, U., 2008. Detrital zircon fingerprint of the proto-Andes: evidence for a Neoproterozoic active margin? *Precambrian Res.* 167, 186–200.
- Chiaradia, M., 2003. The evolution of tungsten sources in crustal mineralization from Archean to Tertiary inferred from lead isotopes. *Econ. Geol.* 98, 1039–1045.
- Clift, P.D., Pecher, I., Kukowski, N., Hampel, A., 2003. Tectonic erosion of the Peruvian forearc, Lima Basin, by subduction and Nazca Ridge collision. *Tectonics* 22 (3), 1–16.
- Cordani, U.G., Sato, K., 2000. Crustal evolution of the South American platform based on Nd isotopic systematics on granitoid rocks. *Episodes* 22, 167–173.
- Corfu, F., Noble, S.R., 1992. Genesis of the southern Abitibi greenstone belt, Superior Province, Canada: evidence from zircon Hf isotope analyses using a single filament technique. *Geochim. Cosmochim. Acta* 56, 2081–2097.
- Couch, R.W., Whitsett, R.M., Briceno, G.L., 1981. Structures of the continental margin of Peru and Chile. *Geological Society of America Memoir* 154, 703–726.
- Davidson, J.P., Arculus, R.J., 2005. The significance of Phanerozoic arc magmatism in generating continental crust. In: Brown, M., Rushmer, T. (Eds.), *Evolution and Differentiation of the Continental Crust*. Cambridge University Press, pp. 135–172.
- Davidson, J.P., Horn, J.M., Garrison, J.M., Dungan, M.A., 2005. Crustal forensics in arc magmas. *J. Volcanol. Geotherm. Res.* 140, 157–170.
- De Bièvre, P., Taylor, P.D.P., 1993. Table of the isotopic composition of the elements. *Int. J. Mass Spectrom. Ion Process.* 123, 149–166.
- de Laeter, J.R., Bukilic, N., 2006. The isotopic composition and atomic weight of ytterbium. *Int. J. Mass Spectrom. Ion Process.* 252, 222–227.
- DePaolo, D.J., 1981. Trace element and isotopic effects of combined wallrock assimilation and fractional crystallization. *Earth Planet. Sci. Lett.* 53, 189–202.
- Dorbath, C., 1996. Velocity structure of the Andes of central Peru from locally recorded earthquakes. *Geophys. Res. Lett.* 23, 205–208.
- Ducea, M.N., Barton, M.D., 2007. Igniting flare-up events in Cordilleran arcs. *Geology* 35, 1047–1050.
- Finch, R.J., Hanchar, J.M., 2003. In: Hanchar, J.M., Hoskin, P.W.O. (Eds.), *Structure and Chemistry of Zircon and Zircon-group Minerals*. Reviews in Mineralogy and Geochemistry, 53, pp. 1–25.
- Franz, G., Lucassen, F., Kramer, W., Trumbull, R.B., Romer, R.L., Wilke, H.-G., Viramonte, J.G., Becchio, R., Siebel, W., 2008. Crustal evolution at the central Andean continental margin: a geochemical record of crustal growth, recycling and destruction. In: Oncken, O., Chong, G., Franz, G., Giese, P., Götze, H.-J., Ramos, V.A., Strecker, M.R., Wigger, P. (Eds.), *The Andes: Active Subduction Orogeny*, 592 p. Springer, Berlin-Heidelberg, pp. 45–64.
- Frost, C.D., Bell, J.M., Frost, B.R., Chamberlain, K.R., 2001. Crustal growth by magmatic underplating: isotopic evidence from the northern Sherman batholith. *Geology* 29, 515–518.
- Gao, S., Luo, T.-C., Zhang, B.-R., Zhang, H.-F., Han, Y.-w., Zhao, Z.-D., Yu, Y.-k., 1998. Chemical composition of the continental crust as revealed by studies in East China – evidence for a 3.0 Ga continental craton. *Geochim. Cosmochim. Acta* 62, 1959–1975.
- Geraldes, M.C., Bettencourt, J.S., Teixeira, W., Matos, J.B., 2004. Geochemistry and isotopic constraints on the origin of the Mesoproterozoic Rio Branco 'anorogenic' plutonic suite, SW of Amazonian craton, Brazil: high heat flow and crustal extension behind the Santa Helena arc? *J. South Am. Earth Sci.* 17, 195–208.
- Graeber, F.M., Asch, G., 1999. Three-dimensional models of P wave velocity and P-to-S velocity ratio in the southern central Andes by simultaneous inversion of local earthquake data. *J. Geophys. Res.* 104 (9), 20237–20256.
- Griffin, W.L., Pearson, N.J., Belousova, E., Jackson, S.E., van Achenbergh, E., O'Reilly, S.Y., Shee, S.R., 2000. The Hf isotope composition of cratonic mantle: LAM-MC-ICPMS analysis of zircon megacrysts in kimberlites. *Geochim. Cosmochim. Acta* 64, 133–147.
- Griffin, W.L., Wang, X., Jackson, S.E., Pearson, N.J., O'Reilly, S.Y., Xu, X., Zhou, X., 2002. Zircon chemistry and magma mixing, SE China: in-situ analysis of Hf isotopes, Tonglu and Pingtan igneous complexes. *Lithos* 61, 237–269.
- Hanchar, J.M., Rudnick, R.L., 1995. Revealing hidden structures: the application of cathodo-luminescence and back-scattered electron imaging to dating zircons from lower crustal xenoliths. *Lithos* 36, 289–303.
- Harris, N.B.W., Pearce, J.A., Tindle, A.G., 1986. Geochemical characteristics of collision-zone magmatism. In: Coward, M.P., Rie, A.C. (Eds.), *Collision Tectonics*. Geological Society, London, vol. 19, pp. 67–81. Special Publication.
- Harris, N.B.W., Hawkesworth, C.J., Tindle, A.G., 1993. The growth of continental crust during the Late Proterozoic: geochemical evidence from the Arabian Shield. *Geol. Soc., London* 76, 363–371 Special Publication.
- Hartley, A.J., Chong, G., Houston, J., Mather, A.E., 2005. 150 million years of climatic stability: evidence from the Atacama Desert, northern Chile. *J. Geol. Soc.* 162, 421–424.
- Haschke, M., Günther, A., 2003. Balancing crustal thickening in arcs by tectonic vs. magmatic means. *Geology* 31, 933–936.
- Hawkesworth, C.J., Kemp, A.I.S., 2006. Evolution of the continental crust. *Nature* 439, 580–583.
- Hildreth, W., Moorbath, S., 1988. Crustal contributions to arc magmatism in the Andes of Central Chile. *Contrib. Mineral. Petrol.* 98, 455–489.
- Hildreth, W., Halliday, A.N., Christiansen, R.L., 1991. Isotopic and chemical evidence concerning the genesis and contamination of basaltic and rhyolitic magma beneath the Yellowstone plateau volcanic field. *J. Petrol.* 32, 63–138.
- Hollister, L.S., Andronicos, C.L., 2006. Formation of new continental crust in Western British Columbia during transpression and transtension. *Earth Planet. Sci. Lett.* 249, 29–38.
- Jahn, B.-M., 2004. The Central Asian Orogenic Belt and growth of the continental crust in the Phanerozoic. *Geol. Soc., London* 226, 73–100 Special Publication.
- Jaillard, E., Hérail, G., Monfret, T., Díaz-Martínez, E., Baby, P., Lavenu, A., Dumont, J.F., 2000. Tectonic evolution of the Andes of Ecuador, Peru, Bolivia and northernmost Chile. In: Cordani, U., Milani, E.J., Thomaz Filho, A., Campos Neto, M.C. (Eds.), *Tectonic Evolution of South America: 31st International Geological Congress, Rio de Janeiro*, pp. 481–559.
- Jull, W., Kelemen, P.B., 2001. On the conditions for lower crustal convective instability. *J. Geophys. Res.* 106, 6423–6446.
- Kelemen, P.B., Yogodzinski, G.M., Scholl, D.W., 2003. Along-strike variation in lavas of the Aleutian island arc: implications for the genesis of high Mg# andesite and the continental crust. In: Eiler, J. (Ed.), *Inside the Subduction Factory*, American Geophysical Union Monograph, vol. 138, pp. 223–246.
- Kinny, P.D., 1986. 3820 Ma zircons from a tonalitic Armiq gneiss in the Godthåb district of Southern West Greenland. *Earth Planet. Sci. Lett.* 79, 337–347.

- Kinny, P.D., Maas, R., 2003. In: Hanchar, J.M., Hoskin, P.W.O. (Eds.), Lu–Hf and Sm–Nd Isotope Systems in Zircon. *Reviews in Mineralogy and Geochemistry*, vol. 53, pp. 327–341.
- Kley, J., Monaldi, C.R., 1998. Tectonic shortening and crustal thickness in the Central Andes; how good is the correlation? *Geology* 26, 723–726.
- Kramers, J.D., Tolstikhin, I.N., 1997. Two terrestrial lead isotope paradoxes, forward transport modelling, core formation and the history of the continental crust. *Chem. Geol.* 139, 75–110.
- Lamb, S.H., Hoke, L., 1997. Origin of the high plateau in the Central Andes, Bolivia, South America. *Tectonics* 16, 623–649.
- Lapen, T.J., Mahlen, N.J., Johnson, C.M., Beard, B.L., 2004. High precision Lu and Hf isotope analyses of both spiked and unspiked samples: a new approach. *Geochem. Geophys. Geosyst.* 5. doi:10.1029/2003/GC000058.
- Lucassen, F., Trumbull, R., Franz, G., Creixell, C., Vasquez, P., Romer, R.L., Figueroa, O., 2004. Distinguishing crustal recycling and juvenile additions at active continental margins: the Paleozoic to recent compositional evolution of the Chilean Pacific margin (36–41°S). *J. South Am. Earth Sci.* 17, 103–119.
- Macfarlane, A.W., Tosdal, R.M., Vidal, C., Paredes, J., 1999. Geologic and isotopic constraints on the age and origin of auriferous-quartz veins in the Parcoy mining district, Pataz, Perú. In: Skinner, B.J. (Ed.), *Geology and Ore Deposits of the Central Andes*, Society of Economic Geologists, vol. 7, pp. 267–279. Special Publication.
- Mégard, F., 1978. Étude géologique des Andes du Pérou central; contribution à l'étude géologique des Andes. *Mémoires de l'ORSTOM*, vol. 86, p. 310.
- Meert, J.G., 2003. A synopsis of events related to the assembly of eastern Gondwana. *Tectonophysics* 362, 1–40.
- Miller, H., Söllner, F., 2005. The Famatina complex (NW Argentina): back-docking of an island arc or terrane accretion? Early Palaeozoic geodynamics at the western Gondwana margin. *Geol. Soc., London* 246, 241–256 Special Publication.
- Mišković, A., Schaltegger, U., Chew, D.M., 2005. Carboniferous plutonism along the Eastern Peruvian Cordillera: implications for the Late Paleozoic to Early Mesozoic Gondwanan tectonics. 6th International Symposium on Andean Geodynamics (ISAG Barcelona), IRD Editions (Institut de Recherche pour le Développement) Paris, pp. 508–511.
- Miskovic, A., Schaltegger, U., Spikings, R.A., Chew, D.M., Kosler, J., Ulianov, A., 2009. Tectonomagmatic evolution of Western Amazonia: geochemical characterization and zircon U–Pb geochronologic constraints from the Peruvian Eastern Cordilleran granitoids. *Geol. Soc. Amer. Bull.* doi:10.1130/B26488.1.
- Mo, X., Nui, Y., Dong, G., Zhao, Z., Hou, Z., Zhou, S., Ke, S., 2008. Contribution of synclinal felsic magmatism to continental crust growth: a case study of the Paleogene Linzizong volcanic succession in southern Tibet. *Chem. Geol.* 250, 49–67.
- Norrish, K., Chappel, B.W., 1967. X-ray fluorescence spectrography. In: Zussman, J. (Ed.), *Physical methods in determinative mineralogy*. New York, Academic Press, pp. 161–214.
- Nowell, G.M., Kempton, P.D., Noble, S.R., Fitton, J.G., Saunders, A.D., Mahoney, J.J., Taylor, R.N., 1998. High precision Hf isotope measurements of MORB and OIB by thermal ionisation mass spectrometry: insights into the depleted mantle. *Chem. Geol.* 149, 211–233.
- Patchett, P.J., Samson, S.D., 2003. Ages and growth of the continental crust from radiogenic isotopes. In: Rudnick, R.L. (Ed.), *The Crust, Treatise on Geochemistry* 3. Elsevier–Pergamon, Oxford, pp. 321–348.
- Patchett, P.J., Tatsumoto, M., 1981. A routine high-precision method for Lu–Hf isotope geochemistry and chronology. *Contrib. Mineral. Petrol.* 75, 263–267.
- Pearce, J.A., Harris, N.B.W., Tindle, A.G., 1984. Trace element discrimination diagrams for the tectonic interpretation of granitic rocks. *J. Petrol.* 25, 956–983.
- Petford, N., Atherton, M.P., Halliday, A.N., 1996. Rapid magma production rates, underplating and remelting in the Andes: isotopic evidence from northern-central Peru (9–11°S). *J. South Am. Earth Sci.* 9, 69–78.
- Plank, T., 2005. Constraints from thorium/lanthanum on sediment recycling at subduction zones and the evolution of the continents. *J. Petrol.* 46, 921–944.
- Polliand, M., Schaltegger, U., Frank, M., Fontboté, L., 2005. Formation of intra-arc volcanosedimentary basins in the western flank of the central Peruvian Andes during Late Cretaceous oblique subduction: field evidence and constraints from U–Pb ages and Hf isotopes. *Int. J. Earth Sci.* 94, 231–242.
- Ramos, V.A., Aleman, A., 2000. Tectonic evolution of the Andes. In: Cordani, U., Milani, E.J., Thomaz Filho, A., Campos Neto, M.C. (Eds.), *Tectonic Evolution of South America: 31st International Geological Congress, Rio de Janeiro*, pp. 635–685.
- Rapalini, A.E., 2005. The accretionary history of southern South America from the latest Proterozoic to the Late Palaeozoic: some palaeomagnetic constraints. *Geol. Soc., London* 246, 305–328 Special Publication.
- Rea, D.K., Ruff, L.J., 1996. Composition and mass flux of sediment entering the world's subduction zones: implications for global sediment budgets, great earthquakes, and volcanism. *Earth Planet Sci Lett* 140, 1–12.
- Reymer, A., Schubert, G., 1984. Phanerozoic addition rates to the continental crust and crustal growth. *Tectonics* 3, 63–77.
- Reynolds, R.C., 1967. Estimation of mass absorption coefficient. *Am. Mineral.* 58, 1069–1072.
- Rudnick, R.L., 1995. Making continental crust. *Nature* 378, 571–578.
- Rudnick, R.L., Gao, S., 2003. Composition of the continental crust. In: Rudnick, R.L. (Ed.), *The Crust, Treatise on Geochemistry* 3. Elsevier–Pergamon, Oxford, pp. 1–64.
- Scholl, D.W., von Huene, R., 2007. Crustal recycling at modern subduction zones applied to the past-issues of growth and preservation of continental basement crust, mantle geochemistry, and supercontinent reconstruction. In: Hatcher, R.D., Carlson, M.P., McBride, J.H., Martínez Catalán, J.R. (Eds.), *4-D Framework of Continental Crust*, Geological Society of America Memoir, 200, pp. 9–32.
- Sguigna, A.P., Larabee, A.J., Waddington, J.C., 1982. The half-life of ¹⁷⁶Lu by a γ – γ coincidence measurement. *Can. J. Phys.* 60, 361–364.
- Slama, J., Košler, J., Condon, D.J., Crowley, J.L., Gerdes, A., Hanchar, J.M., Horstwood, M.S.A., Morris, G.A., Lutz, N., Norberg, N., Schaltegger, U., Schoene, B., Tubrett, M.N., Whitehouse, M.J., 2008. Plešovice zircon – a new natural reference material for U–Pb and Hf isotopic microanalysis. *Chem. Geol.* 249, 1–35.
- Spikings, R.A., Winkler, W., Seward, D., Handler, R., 2001. Along-strike variations in the thermal and tectonic response of the continental Ecuadorian Andes to the collision with heterogeneous oceanic crust. *Earth Planet. Sci. Lett.* 186, 57–73.
- Takahashi, N., Kodaira, S., Klempere, L.S., Tatsumi, Y., Kaneda, Y., Suyehiro, K., 2007. Crustal structure and evolution of the Mariana intra-oceanic island arc. *Geology* 35, 203–206.
- Taylor, S.R., 1977. Island arc models and the composition of the continental crust. In: Talwani, M., Pitman III, W.C. (Eds.), *Island Arcs, Deep Sea Trenches, and Back-Arc Basins*, Maurice Ewing Ser. 1, AGU, Washington, D.C., pp. 325–335.
- Vallejo, C., Spikings, R.A., Luzieux, L., Winkler, W., Chew, D.M., Page, L., 2006. The early interaction between the Caribbean Plateau and the NW South American Plate. *Terra Nova* 18, 264–269.
- Walawender, M.J., Gastel, R.G., Clinkenbeard, J.P., McCormick, W.V., Eastman, B.G., Wernicke, R.S., Wardlaw, M.S., Gunn, S.H., Smith, B.M., 1990. Origin and evolution of the zoned La Posta-type plutons, eastern Peninsular Ranges Batholith, southern and Baja California. In: Anderson, J.L. (Ed.), *The Nature and Origin of Cordilleran Magmatism*, Geological Society of America Memoir, vol. 174, pp. 1–18.
- Whitmeyer, S.J., Karlstrom, K.E., 2007. Tectonic model for the Proterozoic growth of North America. *Geosphere* 3, 220–259.
- Wu, Y.-B., Zheng, Y.-F., Zhang, S.-B., Zhao, Z.-F., Wu, F.-Y., Liu, X.-M., 2007. Zircon U–Pb ages and Hf isotope compositions of migmatite from the North Dabie terrane in China: constraints on partial melting. *J. Metamorph. Geol.* 25, 991–1009.
- Yang, J.-H., Wu, F.-Y., Wilde, S.A., Belousova, E., Griffin, W.L., 2008. Mesozoic decratonization of the North China block. *Geology* 36, 467–470.